Intraband magneto-optical properties of magnetic quantum dots

Ivana Savić[*] and Nenad Vukmirović

School of Electronic and Electrical Engineering, University of Leeds, Leeds LS2 9JT, United Kingdom

(Received 29 June 2007; published 7 December 2007)

The intraband optical properties of quantum dots comprising one electron and up to two Mn ions, subjected to an axial magnetic field, have been investigated theoretically using the configuration-interaction method. We have shown that the electron-Mn and the Mn-Mn exchange interaction mechanisms induce splitting of the energy levels for zero magnetic field, and lead to ground-state transitions and anticrossing of the states for finite magnetic fields. This results in the presence of interesting effects in the intraband absorption spectrum, such as the appearance of new absorption lines and anticrossing features, absent in the single-particle spectrum. Our analysis predicts that both the electron–Mn ion and the Mn-Mn exchange interactions may be probed by means of intraband magneto-optical spectroscopy.

I. INTRODUCTION

Self-assembled quantum dots based on II-VI semiconductor materials, doped with a single or few magnetic atoms, have been attracting increasing research attention in the last few years. They offer unique opportunities to study fundamental quantum-mechanical interactions among spins, charges, and photons.

It is currently experimentally possible to introduce a single Mn atom in a CdTe/ZnTe quantum dot,[1] as well as to control the number of carriers in the dot.[2] Splitting of the exciton line in a single-dot photoluminescence spectrum is a beautiful signature of the interaction between the quantum dot charge and the Mn spin.[1,3–6]

Theoretical studies suggest that the strength and type of magnetic order in such dots can be tailored by the number of carriers,[7–10] quantum dot geometry,[11,12] the positions and the number of Mn ions,[13] or by embedding the dot in a microcavity.[14] It is anticipated that the dots could act as voltage-tunable spin filters[15,16] and nanomagnets.[17] Predictions have also been made that it is possible to optically manipulate the state of a Mn ion in the quantum dot.[5,18] All these properties make quantum dots doped with magnetic atoms excellent candidates for applications in the areas of both spintronics and quantum information processing.

On the road toward these exciting applications, for further understanding of the behavior of magnetic quantum dots, new tools for their characterization are certainly desirable. As far as optical techniques are concerned, only the interband optical properties of these dots have been investigated.[1,3,19] It is shown here that intraband magneto-optical spectroscopy is also a powerful tool for probing the interactions in this type of quantum dots. To date, far-infrared magneto-optical spectroscopy has been successfully applied to study the intraband spectrum of single- and few-particle states in electrostatic quantum dots,[20,21] as well as self-assembled InAs/GaAs quantum dots.[22] It has also been used to probe the interaction among electrons and phonons in self-assembled quantum dots,[23,24] and more recently it has been proposed as a technique to investigate spin-orbit effects in parabolic quantum dots.[25,26] In these two cases, interesting features in the intraband absorption spectrum arise due to coupling of the orbital degree of freedom to another degree of freedom (phonons in the first case, spin in the second case). In magnetic quantum dots, coupling occurs between the orbital degree of freedom of electrons and the spin degree of freedom of magnetic ions. Therefore, one expects to see features in the spectrum, as a signature of their mutual interaction. It should be mentioned that these features can be clearly visible in a single-quantum-dot spectrum only. These will be washed out in the spectra involving ensembles of quantum dots, due to nonuniformities in quantum dot size and random positions of Mn atoms in different dots. However, the feasibility of single-dot photoluminescence spectroscopy, and particularly single-dot interband absorption spectroscopy,[27–29] give hope that intraband absorption spectroscopy on a single-dot level will be feasible in the near future.

We present here a theoretical study of intraband magneto-optical properties of quantum dots containing one electron and a few magnetic ions. In Sec. II we briefly describe a theoretical approach based on the configuration-interaction method, used to calculate the energies and absorption of the system considered. In particular, we specify selection rules for the interaction with in-plane and z-polarized electromagnetic fields. Sections III and IV present a detailed investigation of the influence of the electron–Mn ion and the Mn-Mn exchange interactions on the electronic and optical properties of quantum dots doped with one and two Mn ions, respectively. The conclusions of our analysis are summarized in Sec. V.

II. THEORETICAL CONSIDERATIONS

We consider a quantum dot containing one electron and m Mn ions, subjected to an external magnetic field. The Hamiltonian of the system reads[10,16]

$$
\hat{H} = \sum_{i=1}^{n} \sum_{\sigma} E_{i,\sigma} \hat{c}_{i,\sigma}^{\dagger} \hat{c}_{i,\sigma} - \mu_B g_e B \hat{S}_z - \mu_B g_{\mathrm{Mn}} B \sum_{i=1}^{m} \hat{M}_{iz}
$$

$$
- \frac{1}{2} \sum_{i,j=1}^{n} \sum_{l=1}^{m} J_{ij}^{e}(\mathbf{R}_l) [(\hat{c}_{i,\uparrow}^{\dagger} \hat{c}_{j,\uparrow} - \hat{c}_{i,\downarrow}^{\dagger} \hat{c}_{j,\downarrow}) \hat{M}_{lz} + \hat{c}_{i,\downarrow}^{\dagger} \hat{c}_{j,\uparrow} \hat{M}_{l}^{+}
$$

$$
+ \hat{c}_{i,\uparrow}^{\dagger} \hat{c}_{j,\downarrow} \hat{M}_{l}^{-}] + \frac{1}{2} \sum_{i,j=1}^{m} J_{ij}^{m}(|\mathbf{R}_i - \mathbf{R}_j|) \hat{\mathbf{M}}_i \cdot \hat{\mathbf{M}}_j, \tag{1}
$$

where n is the number of lowest single-particle states of the dot accounted for. The first term corresponds to the Hamiltonian of noninteracting electrons, where $E_{i,\sigma}$ is the energy of the ith electron state of the spin σ, and $\hat{c}^\dagger_{i,\sigma}$ ($\hat{c}_{i,\sigma}$) represent creation (annihilation) operators of the electron. The Zeeman energies of an electron and the Mn ions in a magnetic field are given by the second and the third term, respectively, where μ_B is the Bohr magneton, g_e (g_{Mn}) is the electron (Mn ion) g factor, B is the magnetic field along the z axis, and $\hat{S}_z = \Sigma_{i=1}^n \Sigma_\sigma \sigma \hat{c}^\dagger_{i,\sigma} \hat{c}_{i,\sigma}$ ($\hat{M}_{iz}$) is the operator of the z component of spin of the electron (the ith Mn ion). The fourth term accounts for the exchange interaction between electrons and Mn ions. Its first term describes electron and Mn ion spin-conserving scattering processes, while the other two terms account for simultaneous flipping of electrons and Mn spins, which conserves the total spin. The raising and lowering operators of the spin of the ith Mn ion are denoted as $\hat{M}^+_i$ and $\hat{M}^-_i$. The electron-Mn exchange interaction coupling terms are represented as $J^e_{ij}(\mathbf{R}_l) = J_c \psi^*_i(\mathbf{R}_l) \psi_j(\mathbf{R}_l)$, where $\psi_i(\mathbf{R}_l)$ is the wave function of the electron state i at the position $\mathbf{R}_l$ of the lth Mn ion, and J_c is the electron-Mn exchange interaction strength. The last term describes the Mn-Mn exchange interaction. The Mn-Mn exchange interaction coupling terms between Mn ions i and j are given by $J^m_{ij}(|\mathbf{R}_i - \mathbf{R}_j|) = J_0 \exp[-\lambda(|\mathbf{R}_i - \mathbf{R}_j|/a_0 - 1)]$, where J_0 is the nearest-neighbor interaction strength, and a_0 is the lattice constant. The parameter λ determines the strength of the exchange coupling between a Mn ion and its next-nearest neighbor. In the calculation, we used the following values of the aforementioned parameters: $g_e = -1.67$, $g_{Mn} = 2.02$, $J_c = 15$ eV Å^3, $J_0 = 0.5$ meV, $\lambda = 5.1$ (all from Refs. 10 and 16), and $a_0 = 0.65$ nm (from Ref. 30).

The main interest in this paper will be in changes in the intraband magneto-optical spectrum of self-assembled CdTe/ZnTe quantum dots due to the presence of Mn ions. For that purpose, a model for electronic single-particle states that captures the main features of the intraband optical spectrum is necessary. Self-assembled quantum dots typically have much larger dimensions in the lateral direction than in the growth direction. As a consequence, experimental[31–35] and theoretical[35–40] studies suggest that in-plane-polarized radiation causes non-negligible transitions from the ground state only to the pair of first excited states, while z-polarized radiation causes the transitions to higher excited states, which arise due to confinement predominantly in the growth direction. A model that fully reproduces these features is the model of in-plane parabolic confinement potential and quantum well confinement potential in the z direction and it will be therefore used in this work. The confinement potential then may be given as

$$V(\mathbf{r}) = \frac{1}{2}m^*\omega_0^2 r^2 + V(z), \tag{2}$$

where m^* is the effective mass, ω_0 is the angular frequency of the two-dimensional harmonic confinement, and $V(z)$ represents the potential profile of the quantum well structure. In the case of a magnetic field applied parallel to the z axis, the in-plane motion is decoupled from the motion in the z direction, and the eigenfunctions read

$$\psi_{n_z nl}(\mathbf{r}) = \phi_{n_z}(z)\varphi_{nl}(r,\theta). \tag{3}$$

Here, $\phi_{n_z}(z)$ are the eigenfunctions of the confinement potential along the z axis, and $\varphi_{nl}(r,\theta)$ are the eigenfunctions of the in-plane confinement potential (so called Fock-Darwin states), whose energies are given as

$$E_{nl} = (2n + |l| + 1)\hbar\Omega - \frac{1}{2}l\hbar\omega_c, \tag{4}$$

where $n = 0,1,2,\ldots$ and $l = 0, \pm 1, \ldots$ are the principal and azimuthal quantum numbers, respectively, $\Omega^2 = \omega_0^2 + \frac{1}{4}\omega_c^2$, and $\omega_c = eB/m^*$ is the cyclotron frequency. The corresponding wave functions take the following form:

$$\varphi_{nl}(r,\theta) = \frac{1}{a}\sqrt{\frac{n!}{\pi(n+|l|)!}}\left(\frac{r}{a}\right)^{|l|}e^{-r^2/2a^2}L_n^{|l|}\left[\left(\frac{r}{a}\right)^2\right]e^{il\theta}, \tag{5}$$

where $a^2 = \hbar/(m^*\Omega)$ and $L_n^{|l|}(x)$ is a generalized Laguerre polynomial.

For numerical analysis, we consider a CdTe/ZnTe quantum dot. The effective masses of CdTe and ZnTe of $0.106m_0$ (Ref. 9) and $0.13m_0$ (Ref. 41), where m_0 is the free-electron mass, were used in the electronic structure calculation. For the confinement potential in the z direction, the value of the conduction band offset of 0.6 eV was extracted from Ref. 30, as well as the parameters for the strain potential. The angular frequency of the in-plane confinement was taken to be $\hbar\omega_0 = 51.2$ meV. When absorption of in-plane polarization is investigated, a dot with the quantum well width of 2 nm, which can accommodate one quantum well bound state only, is analyzed. A 4.5-nm-wide quantum well which confines two bound states and therefore allows absorption of z-polarized light on transitions between them will also be investigated.

The many-body Hilbert space may be constructed using the basis states represented as $|\psi_\alpha\rangle = |i_1, i_2, \ldots, i_{N_\uparrow}, j_1, j_2, \ldots, j_{N_\downarrow}\rangle|M_{1z}, M_{2z}, \ldots, M_{mz}\rangle$, where $|i_1, i_2, \ldots, i_{N_\uparrow}, j_1, j_2, \ldots, j_{N_\downarrow}\rangle = \hat{c}^\dagger_{i_1,\uparrow}\hat{c}^\dagger_{i_2,\uparrow}\cdots\hat{c}^\dagger_{i_{N_\uparrow},\uparrow}\hat{c}^\dagger_{j_1,\downarrow}\hat{c}^\dagger_{j_2,\downarrow}\cdots\hat{c}^\dagger_{j_{N_\downarrow},\downarrow}|0\rangle$, $|0\rangle$ is the vacuum, and $N_\uparrow(N_\downarrow)$ is the number of spin-up (spin-down) electrons, $N_\uparrow + N_\downarrow = N$ (here $N = 1$).[10] The z component of the spin of a Mn ion may take values $M_{iz} = \pm 1/2, \pm 3/2, \pm 5/2$, $i = 1, \ldots, m$. The total number of the configurations is given by $6^m\binom{2n}{N}$. In the absence of a magnetic field, the total spin ($\hat{\mathbf{F}} = \hat{\mathbf{S}} + \hat{\mathbf{M}}$) is a good quantum number ($[\hat{\mathbf{F}}, \hat{H}] = 0$) {as well as its z component ($[\hat{F}_z, \hat{H}] = 0$)}. With a magnetic field applied along the z axis, only the z component of the total spin is conserved. As a consequence, the Hamiltonian is block diagonal with blocks corresponding to the basis states with a given value of F_z. The diagonalization can therefore be performed in each block separately. In the spirit of the configuration-interaction approach, the many-body states are expressed as superpositions of the basis states described above ($|\Psi\rangle = \Sigma_\alpha c_\alpha|\psi_\alpha\rangle$). The diagonalization of the Hamiltonian matrix with the elements $\langle\psi_\alpha|\hat{H}|\psi_\beta\rangle$ gives the eigen-

vectors that represent expansion coefficients c_α, and the eigenvalues that correspond to the energies of the interacting system.

The Hamiltonian of the electron-light interaction $\hat{H}'$ in the dipole approximation is proportional to the momentum (or coordinate) operators $\Sigma_{j,k=1}^{n}\mathbf{p}_{jk}\hat{c}_j^\dagger\hat{c}_k$ ($\Sigma_{j,k=1}^{n}\mathbf{r}_{jk}\hat{c}_j^\dagger\hat{c}_k$), where $\mathbf{p}_{jk}$ and $\mathbf{r}_{jk}$ represent momentum and coordinate matrix elements on transitions between single-particle states j and k, respectively. The Hamiltonian does not involve the Mn ion or spin degrees of freedom. Therefore, for zero magnetic field, both the total spin and its z component remain conserved in the presence of an optical field in the system ($[\hat{\mathbf{F}},\hat{H}+\hat{H}']=0,[\hat{F}_z,\hat{H}+\hat{H}']=0$). The same conclusion accounts for the z component of the total spin if a magnetic field parallel to the z direction is applied. These conservation laws in fact determine selection rules for optical transitions in the interacting system at zero ($\Delta F=0$ and $\Delta F_z=0$) and finite magnetic fields ($\Delta F_z=0$).

In first-order perturbation theory (Fermi's golden rule), the intensity of absorption on the transition between an initial state i and a final state f is proportional to the momentum (or coordinate) matrix element $\langle f|\Sigma_{j,k=1}^{n}\mathbf{p}_{jk}\hat{c}_j^\dagger\hat{c}_k|i\rangle$ ($\langle f|\Sigma_{j,k=1}^{n}\mathbf{r}_{jk}\hat{c}_j^\dagger\hat{c}_k|i\rangle$). The single-particle matrix elements of raising and lowering momentum operators for circularly polarized optical field $p_{ij}^\pm=\langle i|p^\pm|j\rangle=\langle n_{zi},n_i,l_i|p^\pm|n_{zj},n_j,l_j\rangle$ are represented as[42]

$$p_{ij}^+ = \frac{i\hbar}{a}\delta_{n_{zi},n_{zj}}\delta_{l_i,l_j+1}\begin{cases}+[(1+a_c)\sqrt{n_j}\,\delta_{n_i,n_j-1}+(1-a_c)\sqrt{n_j+l_j+1}\,\delta_{n_i,n_j}], & l_j\geq 0,\\ -[(1+a_c)\sqrt{n_j-l_j}\,\delta_{n_i,n_j}+(1-a_c)\sqrt{n_j+1}\,\delta_{n_i,n_j+1}], & l_j<0,\end{cases} \quad (6)$$

$$p_{ij}^- = \frac{i\hbar}{a}\delta_{n_{zi},n_{zj}}\delta_{l_i,l_j-1}\begin{cases}-[(1+a_c)\sqrt{n_j+1}\,\delta_{n_i,n_j+1}+(1-a_c)\sqrt{n_j+l_j}\,\delta_{n_i,n_j}], & l_j>0,\\ +[(1+a_c)\sqrt{n_j-l_j+1}\,\delta_{n_i,n_j}+(1-a_c)\sqrt{n_j}\,\delta_{n_i,n_j-1}], & l_j\leq 0,\end{cases} \quad (7)$$

where $a_c=\omega_c/(2\Omega)$. The absorption of in-plane-polarized light on transitions between an initial state i and a final state f is then given as[43]

$$A_{if} \sim \frac{1}{2}(N_i-N_f)\left(\left|\langle f|\sum_{j,k=1}^{n}p_{jk}^+\hat{c}_j^\dagger\hat{c}_k|i\rangle\right|^2 + \left|\langle f|\sum_{j,k=1}^{n}p_{jk}^-\hat{c}_j^\dagger\hat{c}_k|i\rangle\right|^2\right), \quad (8)$$

where N_i is the population of the ith many-body state in thermal equilibrium. When considering z-polarized light, it is more convenient to use the matrix elements of the z coordinate between single-particle states,

$$z_{ij} = \langle i|z|j\rangle = \langle n_{zi},n_i,l_i|z|n_{zj},n_j,l_j\rangle$$
$$= \delta_{n_i,n_j}\delta_{l_i,l_j}\int dz\,\phi_{n_{zi}}(z)z\phi_{n_{zj}(z)}. \quad (9)$$

The absorption of z-polarized light on the transition from an initial state i to a final state f then reads

$$A_{if} \sim (N_i-N_f)\left|\langle f|\sum_{j,k=1}^{n}z_{jk}\hat{c}_j^\dagger\hat{c}_k|i\rangle\right|^2. \quad (10)$$

III. DOTS WITH ONE Mn ION

A. Zero magnetic field

Two possible values of the total spin of the system containing one electron and one Mn ion, whose spins are $1/2$ and $5/2$, respectively, are $5/2+1/2=3$ and $5/2-1/2=2$. If the single-particle electronic spectrum is nondegenerate, all energy levels corresponding to the total spin 3 (2) have seven- (five-)fold degeneracy and, hence, the 12-fold degeneracy of the noninteracting system is partially removed.[2,44] However, in a parabolic quantum dot, where additional degeneracies exist due to the specific form of the potential, this accounts only for the states with the dominant contribution of the configurations whose electronic part corresponds to the nondegenerate s orbital. In this case, the weight of the configurations related to other shells is extremely small, due to a relatively weak electron-Mn exchange interaction between them and the s shell configurations. Accordingly, the energies of those sevenfold and fivefold degenerate states obtained from the full calculation are very similar to those obtained analytically from the limited Hilbert space of the s shell configurations $[E_{|0,0\rangle}-5/4J_{ss}(\mathbf{R}_1)$ and $E_{|0,0\rangle}+7/4J_{ss}(\mathbf{R}_1)$, respectively]. As far as energetically higher shells are concerned, each of the $12n$-fold degenerate energies ($n=2,3,\dots$) splits into three energies only, with sevenfold, ($12n-12$)-fold, and fivefold degeneracy, respectively, due to additional degeneracies of the parabolic quantum dot confinement potential.

In the quantum dots considered ($\hbar\omega_0=51.2$ meV, $d=2$ or 4.5 nm), the ground and the first excited states, determined by the s shell configurations, are well separated from other states. We are interested in absorption at zero or relatively low temperatures, when transitions from these states only make a significant contribution to the spectrum. The selection rules for both in-plane and z polarization of an incident optical field impose the conservation of the total spin and its

z component on transitions between many-particle states. On the other hand, in the single-particle picture, optical transitions for in-plane polarization are allowed if the azimuthal quantum number changes by 1, and other quantum numbers are conserved. Therefore, transitions from the ground ($F = 3, F_z = 0, \pm 1, \pm 2, \pm 3$) and the first excited states ($F = 2, F_z = 0, \pm 1, \pm 2$) may occur only into the states belonging to the same state space $|F, F_z\rangle$ with dominant configurations related to the two degenerate p shell single-particle states. Consequently, for zero temperature, two lines may be observed in the optical spectrum, while for low temperatures when only the ground and the first excited states are populated, up to four lines may appear. In contrast, in the single-particle description, a z-polarized electromagnetic field can induce transitions only between the states with the quantum numbers n_z of opposite parity, and identical principal and azimuthal quantum numbers. Hence, transitions from the ground and the first excited states with the most-weighted configurations associated with the s shell and $n_z = 1$ into the states with the dominant configurations related to the s shell and $n_z = 2$ may contribute to the absorption spectrum. For any value of n_z, the s-like states split into two new ones, with total spins of 3 and 2, and, as a consequence, only one absorption line is present for zero temperature, while another line arises for finite, relatively low, temperatures.

B. Finite magnetic field

The electron-Mn exchange interaction coupling terms $J_{ij}^e(\mathbf{R}_l)$ may be tailored by varying the position of the Mn ions. As discussed earlier, we focus on quantum dots with $d = 2$ and 4.5 nm. In the former case, for a reason that will be explained later, the radial coordinate of a Mn ion is chosen to be 4.5 nm, and the z coordinate is zero (the center of the quantum well). In the latter case, we consider a Mn ion whose radial coordinate is zero, and the z coordinate is taken to be 1.3 nm.

The energy levels of the quantum dot with $d = 2$ nm for all possible values of the z component of the total spin ($F_z = 0, \pm 1, \pm 2, \pm 3$), as they depend on the magnetic field, are shown in Fig. 1(a). The degeneracies present at zero magnetic field are removed upon application of a finite magnetic field, as F is no longer a good quantum number. Since in the system considered F_z is a conserved quantity, the states of different F_z do not interact, and crossing between some of them occurs for certain magnetic fields. On the contrary, the states with the same value of F_z are coupled via the electron-Mn exchange interaction, which leads to their anticrossing if they become almost degenerate for some magnetic fields. A close inspection of the spectrum for several lowest energies for small magnetic fields [see Fig. 1(b)] reveals the ground-state transition from $F_z = 3$ to 2 in an increasing magnetic field. For magnetic fields less than 0.75 T, the ground state is determined by the lowest of the states with the z component of the total spin of $F_z = 3$, with the dominant configuration $|s, \uparrow, 5/2\rangle$. The lowest of the states with $F_z = 2$, whose main components are the configurations $|s, \downarrow, 5/2\rangle$ and $|s, \uparrow, 3/2\rangle$, becomes energetically more favorable for larger magnetic fields. Competing physical mecha-
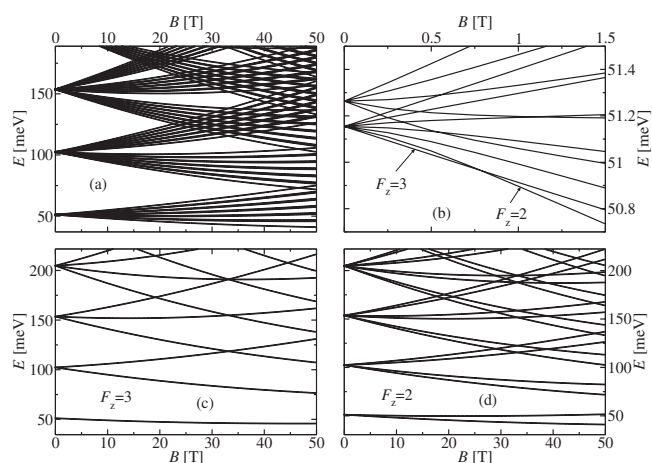
FIG. 1. Energy spectra of one electron and one Mn ion confined in a CdTe quantum dot with $d = 2$ nm. (a) States with all values of the z component of the total spin F_z. (b) Several lowest states shown in (a). (c) States with $F_z = 3$. (d) States with $F_z = 2$.

nisms underlying the ground-state transition are the Zeeman splitting and the electron-Mn exchange interaction, the latter being dominant for small magnetic fields before the transition occurs.

The energy spectra in a magnetic field of the quantum dot with $d = 2$ nm for $F_z = 3$ and 2 are given in Figs. 1(c) and 1(d), respectively. In the case of $F_z = 3$, the lowest state, with the dominant configuration $|s, \uparrow, 5/2\rangle$, is followed by states with the dominant configurations $|i, \uparrow, 5/2\rangle$ ($i = p_1, p_2, d_1, d_2, d_3, \ldots$), and mixing between some of them is prominent only in the vicinity of their crossing point. For example, an increasing magnetic field induces a transformation of nearly pure states $|p_2, \uparrow, 5/2\rangle$ and $|d_1, \uparrow, 5/2\rangle$ to highly mixed states in the basis of these configurations as their energy difference decreases, which is manifested as an anticrossing of these states in the energy spectrum. Analysis of the coefficients in the configuration-interaction expansion reveals that the energy states with $F_z = 2$ mainly comprise pairs of the configurations $|i, \downarrow, 5/2\rangle$ and $|i, \uparrow, 3/2\rangle$ ($i = p_1, p_2, d_1, d_2, d_3, \ldots$) unless some of them become energetically close for certain magnetic fields. Mixing of the configurations $|i, \downarrow, 5/2\rangle$ and $|i, \uparrow, 3/2\rangle$ in a relevant state is more prominent for small magnetic fields, when the Zeeman splitting is comparable to the electron-Mn exchange interaction. However, the Zeeman splitting becomes more important for larger magnetic fields, which results in a weaker coupling of these configurations and one of them becomes prevalent, e.g., the dominant fraction in the lowest state with $F_z = 2$ is that of the configuration $|s, \downarrow, 5/2\rangle$. Again, mixing of states with a dominant influence of configurations associated with different electronic shells is considerable for magnetic fields close to their intersection point.

The optical absorption spectrum of in-plane-polarized light for the quantum dot with $d = 2$ nm at zero temperature is given in Fig. 2(a), with a focus on magnetic fields for which an anticrossing of states occurs and small magnetic fields, shown in Figs. 2(b) and 2(c), respectively. In these, and all the figures that follow, the size of the points is logarithmi-
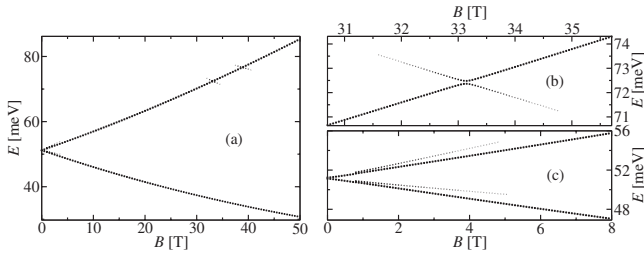
FIG. 2. (a) Absorption spectrum of one electron and one Mn ion confined in a CdTe quantum dot with $d=2$ nm for zero temperature. (b) An anticrossing feature. (c) Additional absorption lines for small magnetic fields.

FIG. 3. Absorption spectrum of one electron and one Mn ion confined in a CdTe quantum dot with $d=2$ nm for a temperature of 10 K. (a) An anticrossing feature. (b) Additional absorption lines for small magnetic fields.

cally (with base 2) proportional to the absorption intensity. At zero temperature, only transitions from the ground state are observable. For $B<0.75$ T, when the ground state is $|s,\uparrow,5/2\rangle$ and optical transitions are restricted to $F_z=3$, the absorption spectrum consists of two branches, which correspond to transitions from $|s,\uparrow,5/2\rangle$ to $|p_1,\uparrow,5/2\rangle$ and $|p_2,\uparrow,5/2\rangle$. For $B>0.75$ T, it comprises four lines, due to the fact that the participating energy levels are mixtures of the states $|i,\downarrow,5/2\rangle$ and $|i,\uparrow,3/2\rangle$, where $i=s,p_1,p_2$. The appearance of additional absorption lines represents a direct manifestation of the role of the electron-Mn exchange interaction and a fingerprint of the ground-state transition driven by the magnetic field. However, for larger magnetic fields, more influential Zeeman splitting leads to decreasing contributions of one of the configurations $|i,\downarrow,5/2\rangle$ and $|i,\uparrow,3/2\rangle$ in each mixed state. As a consequence, the ground state is mainly determined by the configuration $|s,\downarrow,5/2\rangle$, from which optical transitions are allowed only to the states with a dominant influence of the configurations $|p_1,\downarrow,5/2\rangle$ and $|p_2,\downarrow,5/2\rangle$. Therefore, the intensities of two absorption branches which correspond to transitions from the ground state $|s,\downarrow,5/2\rangle$ to the states determined by the configurations $|p_1,\uparrow,3/2\rangle$ and $|p_2,\uparrow,3/2\rangle$ become very weak, leading to their imperceptibility in the absorption spectrum. Furthermore, in the range of magnetic fields between 30 and 40 T, the optical spectrum shows two anticrossing features. This effect originates from mixing of the configurations $|p_2,\downarrow,5/2\rangle$ and $|d_1,\downarrow,5/2\rangle$ ($|p_2,\downarrow,5/2\rangle$ and $|d_1,\uparrow,3/2\rangle$) in the states that intersect for magnetic fields around 33 (39) T. Since the selection rules allow transitions from the configuration $|s,\downarrow,5/2\rangle$ to $|p_2,\downarrow,5/2\rangle$, whose weight in each pair of the intersecting states is considerable, transitions from the ground state to all of these states are observable. The anticrossing splitting energies are ~ 0.12 and ~ 0.1 meV for magnetic fields of 33 and 39 T, respectively, and are very similar to the values $5/2J_{p_2d_1}(\mathbf{R}_1)$ and $\sqrt{5}J_{p_2d_1}(\mathbf{R}_1)$, obtained analytically from the restricted spaces of states $\{|p_2,\downarrow,5/2\rangle,|d_1,\downarrow,5/2\rangle\}$ and $\{|p_2,\downarrow,5/2\rangle,|d_1,\uparrow,3/2\rangle\}$, respectively. In fact, the position of the Mn ion was chosen to maximize the electron–Mn ion exchange interaction coupling term $J_{p_2d_1}(\mathbf{R}_1)$, and hence maximize the anticrossing energies. These results suggest that intraband magneto-optical spectroscopy of quantum dots with one electron and one Mn ion could offer a route for probing the electron-Mn exchange interaction strength.
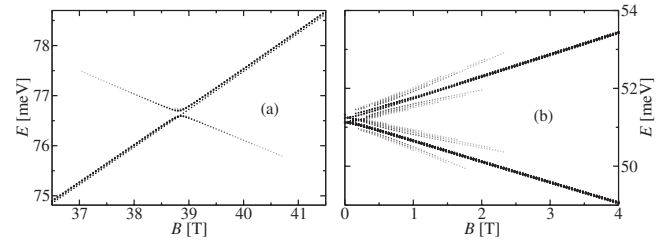
Next we examine the influence of temperature on the absorption spectrum of in-plane-polarized light. The energy spectrum for the states with $F_z=-3$ is qualitatively similar to the one for the states of $F_z=3$ and for each of them, the dominant component is one of the configurations $|i,\downarrow,-5/2\rangle$ ($i=s,p_1,p_2,d_1,d_2,d_3,\dots$). Analogously, the number of energy levels with $F_z=-2,-1,0,1$ is the same as for $F_z=2$ and their dependences on the magnetic field show a similar trend. Under the assumption that the temperature is small enough so that the only states populated are the states of each F_z with the dominant contribution of the s-shell-related configurations, two absorption lines might appear due to transitions between the states with $F_z=3$ or -3, while, for each of the values $F_z=0,\pm1,\pm2$, eight lines may become observable: 44 lines in total.

Figures 3(a) and 3(b) show the magneto-optical spectra of in-plane-polarized radiation for the quantum dot with $d=2$ nm at the temperature of $T=10$ K in the range of magnetic fields for which the second anticrossing occurs and small magnetic fields, respectively. In the latter case, the Zeeman splitting of the s-shell-related states is not so pronounced, resulting in a larger number of lines. Due to the fact that a certain fraction of the total population does not reside on the ground state, the two weaker absorption modes from the ground state present at zero temperature have smaller intensities for finite temperatures [compare Figs. 2(c) and 3(b)]. Instead of the two strong intensity lines characteristic for zero temperature, now there are additional weaker intensity modes in their vicinity throughout the range of magnetic fields considered. We observe that the signature of optical transitions from the ground state with $F_z=2$ to the two states that anticross at a magnetic field of 39 T persists in the absorption spectrum for the temperature of 10 K. Furthermore, the line assigned to transitions from the lowest state with $F_z=3$ to the state with the dominant configuration $|p_2,\uparrow,5/2\rangle$ is clearly visible [see Fig. 3(a)], since the latter does not experience anticrossing with any of the states with $F_z=3$ [see Fig. 1(c)]. On the contrary, for a magnetic field of 33 T, this line is not present, due to the repulsion of the states $|p_2,\uparrow,5/2\rangle$ and $|d_1,\uparrow,5/2\rangle$, resulting in an anticrossing feature in the absorption spectrum which simply adds to the one for the states with $F_z=2$.

In the following, we turn our attention to absorption in the case of z-polarized incident light. We consider a quantum dot with $d=4.5$ nm which can also accommodate bound states
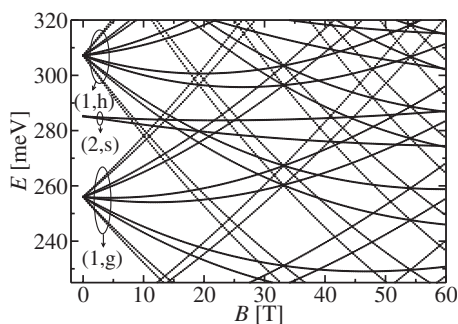
FIG. 4. Energy spectrum of one electron and one Mn ion confined in a CdTe quantum dot with $d=4.5$ nm for states with the z component of the total spin $F_z=2$.

with $n_z=2$. An applied magnetic field induces the same ground-state transition as discussed in the case of the quantum dot with $d=2$ nm (from $F_z=3$ to 2). Figure 4 shows the magnetic field dependence of the energy levels with the z component of the total spin of $F_z=2$. For zero magnetic field, the states related to the configurations $|2,s,\downarrow,5/2\rangle$ and $|2,s,\uparrow,3/2\rangle$ are located between the states associated with the pairs of the configurations $\{|1,g_i,\downarrow,5/2\rangle,|1,g_i,\uparrow,3/2\rangle\}$, $1\leq i\leq 5$, and $\{|1,h_i,\downarrow,5/2\rangle,|1,h_i,\uparrow,3/2\rangle\}$, $1\leq i\leq 6$. The energy spectrum of the states with $F_z=3$ exhibits the main characteristics of the corresponding spectrum for the quantum dot with $d=2$ nm. Additionally, it includes higher energy levels, with prominent contributions of the configurations related to the single-particle states with $n_z=2$.

For $B<1.5$ T, when the state $|1,s,\uparrow,5/2\rangle$ represents the ground state of the system, only one line emerges in the absorption spectrum, shown in Fig. 5(b), and it is related to transitions from the ground state into the state $|2,s,\uparrow,5/2\rangle$. The presence of two absorption lines for zero temperature and small magnetic fields after the ground-state transition [see Fig. 5(b)] originates from the fact that the configurations $|2,s,\downarrow,5/2\rangle$ and $|2,s,\uparrow,3/2\rangle$ represent the largest components of the state into which optical transitions from the ground state, determined by the configurations $|1,s,\downarrow,5/2\rangle$ and $|1,s,\uparrow,3/2\rangle$, may occur. As described in the case of in-plane polarization, one of the two configurations in each of these states becomes of minor importance in an increasing magnetic field and, hence, one of the absorption lines almost disappears from the optical spectrum. Despite a significant number of intersections of the states comprising $|2,s,\downarrow,5/2\rangle$
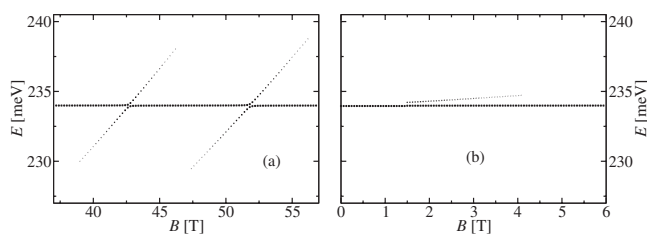
FIG. 5. Absorption spectrum of one electron and one Mn ion confined in a CdTe quantum dot with $d=4.5$ nm at zero temperature. (a) An anticrossing feature. (b) Additional absorption lines for small magnetic fields.

and $|2,s,\uparrow,3/2\rangle$ with the states associated with the single-particle states with the quantum number $n_z=1$, only two anticrossing structures are visible in the absorption spectrum (~ 0.18 meV for $B\approx 43$ T and ~ 0.21 meV for $B\approx 52$ T); see Fig. 5(a). The origin of this effect is the choice of the position of the Mn ion (zero radial coordinate), with a purpose of increasing the electron–Mn ion exchange coupling between the single-particle states $|2,s\rangle$ and $|1,g_3\rangle$. Consequently, the electron-Mn exchange matrix elements between the configurations related to $|2,s\rangle$ and $|1,i\rangle$, $i\neq g_3$, are zero, and hence there is no interaction between the states whose main ingredients are these configurations. For relatively low temperatures, one (four) lines may appear in the absorption spectrum in transitions between the states with one of the values $F_z=\pm 3$ ($F_z=0,\pm 1,\pm 2$), resulting in the total number of lines of 22.

IV. DOTS WITH TWO Mn IONS

A. Zero magnetic field

The total spin of the system with one electron and two Mn ions can take the following values: $1/2$, $3/2$, $5/2$, $7/2$, and $9/2$; $1/2$, $3/2$, $5/2$, $7/2$, $9/2$, and $11/2$; and the corresponding energy levels have two-, four-, six-, eight-, and tenfold; two-, four-, six-, eight-, ten-, and 12-fold degeneracy, respectively. More degeneracies emerge in a quantum dot with distant, nearly noninteracting Mn ions, because of the degenerate single-particle spectrum. However, this situation is changed if the distance between the Mn ions is sufficiently small so that a considerable Mn-Mn exchange interaction lifts some of those degeneracies. In either case, the single-particle ground state splits into 11 energy levels, with the most-weighted configurations associated with the s shell. At zero temperature only two modes exist in the absorption spectrum of in-plane-polarized light, due to transitions from the s-shell-like degenerate ground state to the states related to the p shell configurations of the same total spin and its z component. For the same reason, at a finite temperature facilitating occupation of those 11 lowest energy levels only, the maximum number of 22 modes could be detected. At zero temperature, the optical spectrum of z-polarized light includes one line associated with transitions from the ground state to the state with the dominant configuration related to the s shell and $n_z=2$ with the same F and F_z, and the number of lines amounts to 11 as the temperature increases.

B. Finite magnetic field

1. Noninteracting Mn ions

A quantum dot with $d=2$ nm, one electron, and two diametrally opposite Mn ions, with the radial coordinate of 4.5 nm and zero z coordinate, is of interest in the following. The energy spectrum of the system with one electron and two Mn ions exhibits a richer structure than the one with only one Mn ion. It includes 72 states stemming from each single-particle state; in comparison, the system with only one Mn ion comprises 12 such states. The system undergoes the ground-state transition at a magnetic field of 1.5 T, from the state $|s,\uparrow,5/2,5/2\rangle$ with $F_z=11/2$ to the state with
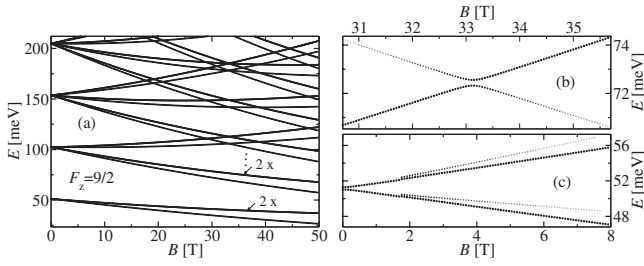
FIG. 6. (a) Energy spectrum of one electron and two noninteracting Mn ions confined in a CdTe quantum dot with $d=2$ nm for states with the z component of the total spin $F_z=9/2$. The states marked with $2\times$ are twofold degenerate for magnetic fields larger than 3 T. The corresponding optical absorption spectrum at zero temperature: (b) an anticrossing feature; (c) additional absorption lines for small magnetic fields.

$F_z=9/2$ consisting mainly of the configurations $|s,\downarrow,5/2,5/2\rangle$, $|s,\uparrow,5/2,3/2\rangle$, and $|s,\uparrow,3/2,5/2\rangle$. Apart from a different Zeeman shift due to the presence of another Mn ion and different anticrossing splittings, the electronic structure of the parabolic quantum dot with two noninteracting Mn ions for $F_z=11/2$ shows a close resemblance to the one with one Mn ion for $F_z=3$ [see Fig. 1(c)]. However, the dependences of the energies of the states with $F_z=9/2$ on the magnetic field, depicted in Fig. 6(a), are not analogous to those of one Mn ion for $F_z=2$. The contribution of the configuration $|s,\downarrow,5/2,5/2\rangle$ to the lowest state with $F_z=9/2$ becomes dominant in an increasing magnetic field. The subsequent two energy levels, comprising the configurations $|s,\uparrow,5/2,3/2\rangle$ and $|s,\uparrow,3/2,5/2\rangle$, are nearly degenerate for larger magnetic fields [marked in Fig. 6(a)], due to an inconsiderable Mn-Mn exchange interaction between the symmetrically positioned Mn ions. For smaller magnetic fields ($B<3$ T), these degeneracies are lifted, as a result of a relatively strong electron–Mn ion exchange interaction among the configurations $|s,\downarrow,5/2,5/2\rangle$, $|s,\uparrow,5/2,3/2\rangle$, and $|s,\uparrow,3/2,5/2\rangle$. A similar situation occurs for states involving configurations related to the other orbitals. Consequently, no additional anticrossing of states is manifested in the spectrum in comparison to the case of one Mn ion.

The absorption spectrum at zero temperature and for the system of one electron and two noninteracting Mn ions is almost equivalent to the one for one electron and only one Mn ion with two times stronger electron-Mn exchange interaction strength J_c, for both in-plane- and z-polarized optical field. In the case of in-plane polarization [see Figs. 6(b) and 6(c)], the optical spectrum shows evidence of the excitation of electrons from the state $|s,\uparrow,5/2,5/2\rangle$ to the states $|p_1,\uparrow,5/2,5/2\rangle$ and $|p_2,\uparrow,5/2,5/2\rangle$ up to $B=1.5$ T. Subsequently, only electrons from the ground state of $F_z=9/2$, whose major constituents are $|s,\downarrow,5/2,5/2\rangle$, $|s,\uparrow,5/2,3/2\rangle$, and $|s,\uparrow,3/2,5/2\rangle$, may be optically activated. This translates into the appearance of two extra lines of a larger intensity than in the case of one Mn ion, which are observable for a wider range of magnetic fields, due to larger mixing of relevant configurations ($|i,\downarrow,5/2,5/2\rangle$, $|i,\uparrow,5/2,3/2\rangle$, and $|i,\uparrow,3/2,5/2\rangle$, for each $i=s,p_1,p_2$). Two times larger anticrossing energies for magnetic fields of
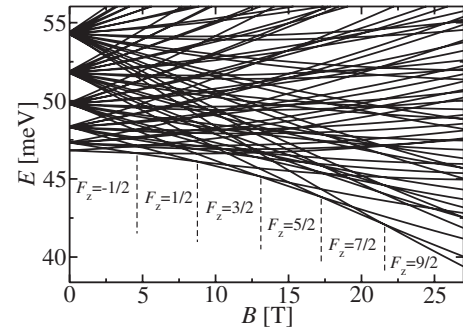
FIG. 7. Several lowest states with all values of the z component of the total spin F_z in the energy spectrum of one electron and two strongly interacting Mn ions confined in a CdTe quantum dot with $d=2$ nm. The values of F_z of the ground state for different magnetic fields are also shown.

33 and 39 T are reflected in the absorption spectra additionally via larger intensities of the lines corresponding to the transitions which would be forbidden in the absence of the electron–Mn ion interaction. The magneto-optical spectrum for finite temperatures includes new, energetically close, modes.

2. Strongly interacting Mn ions

Next we analyze a quantum dot with $d=2$ nm, one electron, and two Mn ions with the same polar and z coordinates ($z=0$), and the radial coordinates of 4.5 and 5.15 nm (Mn ions are separated by one lattice constant). A strong interaction between Mn ions changes the ordering of the states associated with a particular shell at zero magnetic field in comparison to the noninteracting case. As a result, the ground state of the system for small magnetic fields is that of $F_z=-1/2$ as opposed to $F_z=11/2$ for noninteracting Mn ions. Figure 7 illustrates that the ground state experiences multiple transitions from $F_z=-1/2$, via $F_z=1/2$, $3/2$, $5/2$, and $7/2$, to $F_z=9/2$ for increasing magnetic fields, as a consequence of the interplay of the Zeeman splitting and the electron-Mn and the Mn-Mn exchange interactions. Figures 8(a) and 8(b) represent the energy levels versus magnetic field dependences for $F_z=-1/2$ and $9/2$, respectively. Clearly, the Mn-Mn exchange interaction removes previously discussed degeneracies of states present in the system with two noninteracting Mn ions with the same radial coordinate, shown in Fig. 6(a). Also, the choice of the nonidentical radial coordi-
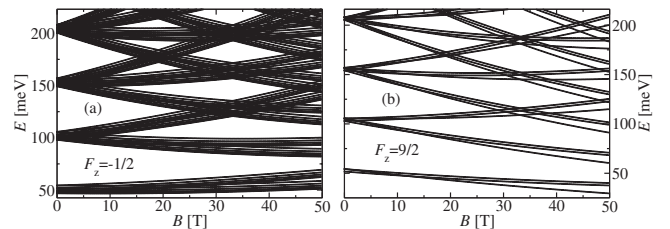
FIG. 8. Energy spectra of one electron and two strongly interacting Mn ions confined in a CdTe quantum dot with $d=2$ nm. (a) States with the z component of the total spin $F_z=-1/2$. (b) States with $F_z=9/2$.
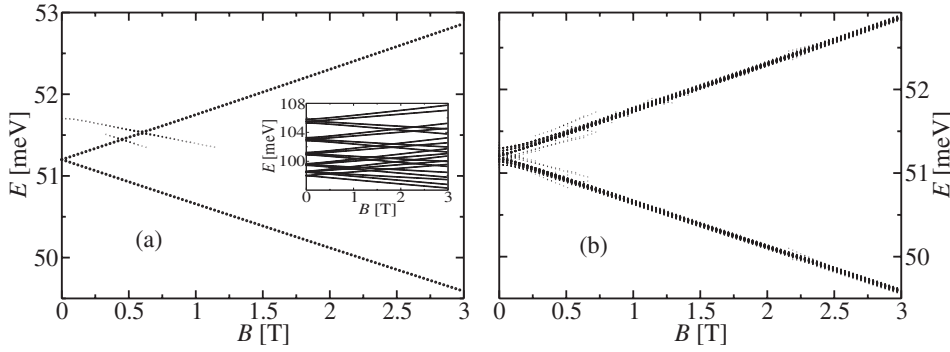
FIG. 9. Absorption spectra of one electron and two strongly interacting Mn ions confined in a CdTe quantum dot with $d=2$ nm. (a) Zero temperature. Inset: States with the z component of the total spin $F_z=-1/2$ related to the p shell as a function of the magnetic field. (b) A temperature of 10 K.

nates for the Mn ions leads to lifting of these degeneracies, but to a much smaller extent than the Mn-Mn exchange interaction.

For large magnetic fields when no crossing of the single-particle states occurs (the electron–Mn ion interaction is insignificant), the states of the system are direct products of the single-particle states with the eigenstates of the operator $-\mu_B g_{Mn}(\hat{M}_{1z}+\hat{M}_{2z})B+J_{12}^m(|\mathbf{R}_1-\mathbf{R}_2|)\hat{\mathbf{M}}_1\cdot\hat{\mathbf{M}}_2$. For instance, the s-orbital-related states with $F_z=9/2$ can be represented approximately as $|s,\downarrow,5/2,5/2\rangle$, $1/\sqrt{2}|s,\uparrow,3/2,5/2\rangle-1/\sqrt{2}|s,\uparrow,5/2,3/2\rangle$, and $1/\sqrt{2}|s,\uparrow,3/2,5/2\rangle+1/\sqrt{2}|s,\uparrow,5/2,3/2\rangle$. In the situations when the electron-Mn exchange interaction is more competitive (for small magnetic fields or in the vicinity of the crossing points of single-particle states), the states may be approximated by linear combinations of appropriate direct products described above. Another novelty in the electronic structure which arises as a consequence of the Mn-Mn exchange interaction is the anticrossing of the states governed by the configurations related to different single-particle states of the same shell (e.g., p_1 and p_2) [see the inset of Fig. 9(a)]. In fact, the Mn-Mn exchange interaction can couple only configurations associated with the same single-particle state, and the actual coupling between the states ascribed to different single-particle states when they become nearly degenerate originates from the electron–Mn ion exchange interaction. However, the Mn-Mn exchange interaction is responsible for the splitting of these many-particle states for zero magnetic field, which leads to their intersection and coupling via the electron–Mn ion exchange interaction for finite magnetic fields.

The magneto-optical spectra of in-plane-polarized optical fields for the quantum dot containing two strongly correlated Mn ions for the temperatures of 0 and 10 K are given in Figs. 9(a) and 9(b), respectively. For almost the entire range of the magnetic fields considered (0–50 T), only two modes related to optical excitations from the ground state into the p_1- or p_2-like states are visible for zero temperature. This is a result of the fact that transitions between states that are direct products between the single-particle states and the eigenstates of the operator $-\mu_B g_{Mn}(\hat{M}_{1z}+\hat{M}_{2z})B+J_{12}^m(|\mathbf{R}_1-\mathbf{R}_2|)\hat{\mathbf{M}}_1\cdot\hat{\mathbf{M}}_2$ are allowed if the latter are identical, as well as if the selection rules for the single-particle states are satisfied. To illustrate this, for $F_z=9/2$, electrons from the ground state $|s,\downarrow,5/2,5/2\rangle$ can be optically excited into $|p_{1,2},\downarrow,5/2,5/2\rangle$, while the transitions into the

states $1/\sqrt{2}|p_{1,2},\uparrow,3/2,5/2\rangle-1/\sqrt{2}|p_{1,2},\uparrow,5/2,3/2\rangle$ and $1/\sqrt{2}|p_{1,2},\uparrow,3/2,5/2\rangle+1/\sqrt{2}|p_{1,2},\uparrow,5/2,3/2\rangle$ are forbidden. A careful inspection of the energy states for $F_z=9/2$ might lead to an expectation that three anticrossing features will arise in the absorption spectrum for magnetic fields between 30 and 40 T. However, only two of them are actually observable. The opposite signs of the coefficients of the state $1/\sqrt{2}|d_1,\uparrow,3/2,5/2\rangle-1/\sqrt{2}|d_1,\uparrow,5/2,3/2\rangle$ almost cancel the contribution of the electron-Mn exchange interaction with the state $|p_2,\downarrow,5/2,5/2\rangle$ at a magnetic field of 36 T and, therefore, no new anticrossing can be detected.

In the range of small magnetic fields when the ground state is the one with $F_z=-1/2$, the absorption spectrum shows signatures of the anticrossing of the states related to configurations with the single-particle states p_1 and p_2, induced by the Mn-Mn exchange interaction, given in Fig. 9(a). For our choice of the Mn ions' positions, the electron-Mn exchange matrix elements between the orbitals p_1 and p_2 are even larger than those between the orbitals p_2 and d_1. Nevertheless, the influence of the electron–Mn ion exchange interaction on the intersecting states associated with the p shell states is counteracted by a strong Mn-Mn exchange interaction. Therefore, despite a significant number of such states, not all of them are coupled sufficiently in the proximity of their crossing points and only two anticrossing characteristics are apparent in the absorption spectrum. Furthermore, the anticrossing energies in this case are an order of magnitude smaller than for magnetic fields between 30 and 40 T ($\sim$0.013 meV for $B=0.44$ T, and $\sim$0.021 meV for $B=0.6$ T). For each of the lowest states belonging to one of the spaces of states with $F_z=1/2$, $3/2$, $5/2$, and $7/2$, the anticrossings of the states associated with p orbitals do not occur within the range of magnetic fields for which that state represents the ground state of the system, and hence are not detectable in the absorption spectrum for zero temperature. However, a finite temperature gives rise to weak signatures of some of them, e.g., for magnetic fields of $\sim$1.4 and $\sim$2.4 T [see Fig. 9(b)]. Thermal activation of electrons decreases the population of the ground state with $F_z=-1/2$, resulting in less distinct anticrossing structures in comparison to those in the absorption spectra for zero temperature [see Figs. 9(a) and 9(b)]. Since the single-particle electronic structure is characterized by one s orbital only, the optical spectrum for z polarization does not exhibit extra anticrossing features attributed to the Mn-Mn exchange interaction. Therefore, its dependence of the magnetic field is very similar to the one with two noninteracting Mn ions.
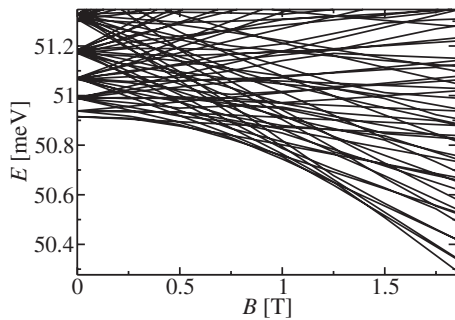
FIG. 10. Several lowest states with all values of the z component of the total spin F_z in the energy spectra of one electron and two weakly interacting Mn ions confined in a CdTe quantum dot with $d=2$ nm.

3. Weakly interacting Mn ions

Finally, we explore magneto-optical properties of a quantum dot with $d=2$ nm confining one electron and two Mn ions with the same polar and zero z coordinates, and radial coordinates of 4.5 and 5.5 nm. Although the Mn-Mn exchange interaction is not so prominent as in the case previously considered, the ground-state transitions from $F_z=-1/2$ to $9/2$ can still be identified in the energy spectrum, shown in Fig. 10. However, the ranges of magnetic fields for which each of these states represents the ground state are significantly smaller compared to the case of the strong interaction (see Fig. 7). The energy states include contributions of all configurations with a particular value of F_z, and not only of those that are coupled by the Mn-Mn exchange interaction. The splitting of the states with a dominant influence of the configurations associated with different states of the same shell is much smaller in comparison to the system with strongly interacting Mn ions and the corresponding anticrossing characteristics are hardly observable for very small magnetic fields.

The optical spectra for in-plane polarization versus magnetic field dependence for small magnetic fields at the temperatures of 0 and 10 K are illustrated in Figs. 11(a) and 11(b), respectively. A weak Mn-Mn exchange interaction
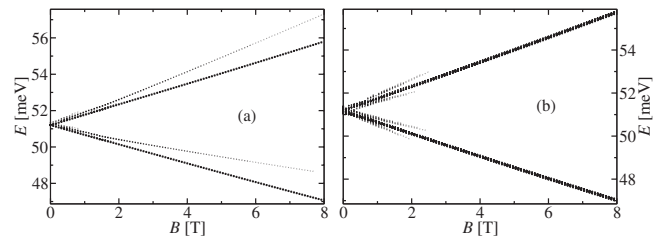
FIG. 11. Absorption spectra of one electron and two weakly interacting Mn ions confined in a CdTe quantum dot with d = 2 nm. (a) Zero temperature. (b) A temperature of 10 K.

gives rise to new absorption lines at zero temperature in comparison to the system with one electron and two strongly interacting Mn ions. The origin of this effect is a larger coupling of relevant configurations via the electron–Mn ion interaction in the states participating in the optical transitions. Discontinuities between optical modes represent an evidence of the multitude of the ground-state transitions. For magnetic fields larger than 2 T, when the ground state is the lowest state of $F_z=9/2$, the absorption spectrum becomes very similar to the one of the two noninteracting Mn ions [see Fig. 6(c)]. In the case of z-polarized optical field, the magneto-optical spectrum is the same as for the system with both strongly interacting and noninteracting Mn ions.

V. CONCLUSION

In summary, we studied the electronic structure and intraband absorption of II-VI quantum dots in a magnetic field, with one electron and one or two Mn ions. Lifting of the degeneracy of the energy levels for zero magnetic field, as well as anticrossing of the states and ground-state transitions in an axial magnetic field, are attributed to the electron-Mn and the Mn-Mn exchange interactions, which may be tailored by an appropriate positioning of the Mn ions. These effects are also reflected in the absorption spectrum via new absorption modes and anticrossing characteristics. This indicates that far-infrared magneto-optical spectroscopy could be employed to examine the role of the electron–Mn ion and the Mn-Mn exchange interaction in quantum dots doped with few Mn ions.

*I.Savic@leeds.ac.uk

[1] L. Besombes, Y. Leger, L. Maingault, D. Ferrand, H. Mariette, and J. Cibert, Phys. Rev. Lett. **93**, 207403 (2004).

[2] Y. Leger, L. Besombes, J. Fernandez-Rossier, L. Maingault, and H. Mariette, Phys. Rev. Lett. **97**, 107401 (2006).

[3] Y. Leger, L. Besombes, L. Maingault, D. Ferrand, and H. Mariette, Phys. Rev. Lett. **95**, 047403 (2005).

[4] L. Besombes, Y. Leger, L. Maingault, D. Ferrand, H. Mariette, and J. Cibert, Phys. Rev. B **71**, 161307(R) (2005).

[5] J. Fernandez-Rossier, Phys. Rev. B **73**, 045301 (2006).

[6] A. K. Bhattacharjee and J. Pérez-Conde, Phys. Rev. B **68**, 045303 (2003).

[7] A. O. Govorov, Phys. Rev. B **72**, 075359 (2005).

[8] J. Fernandez-Rossier and L. Brey, Phys. Rev. Lett. **93**, 117201 (2004).

[9] F. Qu and P. Hawrylak, Phys. Rev. Lett. **95**, 217206 (2005).

[10] F. Qu and P. Hawrylak, Phys. Rev. Lett. **96**, 157201 (2006).

[11] A. K. Bhattacharjee and C. Benoit a là Guillaume, Phys. Rev. B **55**, 10613 (1997).

[12] A. K. Bhattacharjee, Phys. Rev. B **58**, 15660 (1998).

[13] R. M. Abolfath, P. Hawrylak, and I. Žutić, Phys. Rev. Lett. **98**, 207203 (2007).

[14] G. Chiappe, J. Fernandez-Rossier, E. Louis, and E. V. Anda, Phys. Rev. B **72**, 245311 (2005).

[15] F. Qu and P. Vasilopoulos, Appl. Phys. Lett. **89**, 122512 (2006).

[16] F. Qu and P. Vasilopoulos, Phys. Rev. B **74**, 245308 (2006).

[17] J. Fernandez-Rossier and R. Aguado, Phys. Rev. Lett. **98**, 106805 (2007).

[18] A. O. Govorov and A. V. Kalameitsev, Phys. Rev. B **71**, 035338 (2005).

[19] P. Wojnar, J. Suffczyński, K. Kowalik, A. Golnik, G. Karczewski, and J. Kossut, Phys. Rev. B **75**, 155301 (2007).

[20] C. Sikorski and U. Merkt, Phys. Rev. Lett. **62**, 2164 (1989).

[21] B. Meurer, D. Heitmann, and K. Ploog, Phys. Rev. Lett. **68**, 1371 (1992).

[22] M. Fricke, A. Lorke, J. P. Kotthaus, G. Medeiros-Ribeiro, and P. M. Petroff, Europhys. Lett. **36**, 197 (1996).

[23] B. A. Carpenter, E. A. Zibik, M. L. Sadowski, L. R. Wilson, D. M. Whittaker, J. W. Cockburn, M. S. Skolnick, M. Potemski, M. J. Steer, and M. Hopkinson, Phys. Rev. B **74**, 161302(R) (2006).

[24] S. Hameau, Y. Guldner, O. Verzelen, R. Ferreira, G. Bastard, J. Zeman, A. Lemaître, and J. M. Gérard, Phys. Rev. Lett. **83**, 4152 (1999).

[25] P. Pietilainen and T. Chakraborty, Phys. Rev. B **73**, 155315 (2006).

[26] T. Chakraborty and P. Pietilainen, Phys. Rev. Lett. **95**, 136603 (2005).

[27] N. H. Bonadeo, A. S. Lenihan, G. Chen, J. R. Guest, D. G. Steel, D. Gammon, D. S. Katzer, and D. Park, Appl. Phys. Lett. **75**, 2933 (1999).

[28] B. Alén, F. Bickel, K. Karrai, R. J. Warburton, and P. M. Petroff, Appl. Phys. Lett. **83**, 2235 (2003).

[29] S. Seidl, M. Kroner, P. A. Dalgarno, A. Högele, J. M. Smith, M. Ediger, B. D. Gerardot, J. M. Garcia, P. M. Petroff, K. Karrai, and R. J. Warburton, Phys. Rev. B **72**, 195339 (2005).

[30] T. Li, H. J. Lozykowski, and J. L. Reno, Phys. Rev. B **46**, 6961 (1992).

[31] S. Sauvage, P. Boucaud, T. Bruhnes, V. Immer, E. Finkman, and J. M. Gerard, Appl. Phys. Lett. **78**, 2327 (2001).

[32] A. M. Adawi, E. A. Zibik, L. R. Wilson, A. Lemaître, J. W. Cockburn, M. S. Skolnick, M. Hopkinson, and G. Hill, Appl. Phys. Lett. **83**, 602 (2003).

[33] B. Aslan, H. C. Liu, M. Korkusinski, S.-J. Cheng, and P. Hawry-lak, Appl. Phys. Lett. **82**, 630 (2003).

[34] H. C. Liu, Opto-Electron. Rev. **11**, 1 (2003).

[35] F. F. Schrey, L. Rebohle, T. Müller, G. Strasser, K. Unterrainer, D. P. Nguyen, N. Regnault, R. Ferreira, and G. Bastard, Phys. Rev. B **72**, 155310 (2005).

[36] H. Jiang and J. Singh, Appl. Phys. Lett. **71**, 3239 (1997).

[37] J.-Z. Zhang and I. Galbraith, Appl. Phys. Lett. **84**, 1934 (2004).

[38] G. A. Narvaez and A. Zunger, Phys. Rev. B **75**, 085306 (2007).

[39] N. Vukmirović, Ž. Gačević, Z. Ikonić, D. Indjin, P. Harrison, and V. Milanović, Semicond. Sci. Technol. **21**, 1098 (2006).

[40] N. Vukmirović, D. Indjin, Z. Ikonić, and P. Harrison, Appl. Phys. Lett. **88**, 251107 (2006).

[41] J. Li and L.-W. Wang, Phys. Rev. B **72**, 125325 (2005).

[42] F. B. Pedersen and Y.-C. Chang, Phys. Rev. B **55**, 4580 (1997).

[43] T. Chakraborty, V. Halonen, and P. Pietiläinen, Phys. Rev. B **43**, 14289 (1991).

[44] S.-J. Cheng, Phys. Rev. B **72**, 235332 (2005).